

Accepted version on Author's Personal Website: C. R. Koch

Article Name with DOI link to Final Published Version complete citation:

C. Slepicka and C. R. Koch. Iterative learning controller on dual-fuel control of homogeneous charge compression ignition. In *IFAC Advances in Automotive Controls Conference (AAC)*, Sweden, volume 49, pages 347–352. Elsevier, June 2016

See also:

https://sites.ualberta.ca/~ckoch/open_access/Slepicka2016aac.pdf

Post-print

As per publisher copyright is ©2016



This work is licensed under a
[Creative Commons Attribution-NonCommercial-NoDerivatives 4.0 International License](https://creativecommons.org/licenses/by-nc-nd/4.0/).



Article accepted version starts on the next page →

[Or link: to Author's Website](#)

Iterative Learning on Dual-fuel Control of Homogeneous Charge Compression Ignition^{*}

Craig Slepicka^{*} Charles R. Koch^{*}

^{*} *University of Alberta, Edmonton AB T6G 2G8 Canada (e-mail: slepicka@ualberta.ca, bob.koch@ualberta.ca).*

Abstract: An Iterative Learning Controller (ILC) is used to control a dual-fuel Homogeneous Charge Compression (HCCI) engine. The engine is a CFR engine with in-cylinder pressure measurement ports and is operated at 100°C intake heating, 800 RPM and a compression ratio of 11:1. To control combustion timing and load, the amount of iso-octane and n-heptane injected into the manifold are used as inputs. The metrics used for combustion timing and load are CA50, crank angle when 50% of the fuel is burned, and gross IMEP, respectively. Using these inputs and outputs a system identification is performed and an ARMAX model is obtained. This model is then used to generate a norm optimal control. The norm optimal control is compared to a model-less control strategy that involves populating the off-diagonal of the learning matrix using a Jacobian estimate inverse. Both systems are used to follow a reference trajectory involving a step input in IMEP then CA50. The model-less control outperforms the norm optimal in both convergence speed and final iteration error. Application of non-causal filters within the iteration is also tested using a zero-phase filter and a Gaussian filter. The zero-phase has faster convergence than either the Gaussian or filter-less and has better final iteration error. This gives the best ILC control as model-less with zero-phase filter. This control is then compared with two PI controllers. It is found that the ILC outperforms the PI controllers after 3 iterations.

Keywords: Iterative learning controller, Dual-fuel, HCCI.

1. INTRODUCTION

Homogeneous Charge Compression Ignition (HCCI) is an advanced combustion strategy used in internal combustion engines. It allows for increased fuel efficiency, reduced emissions (Iida et al., 2003), and varying fuel selection (Kalghatgi and Head, 2004). The downside is the lack of direct control of ignition timing, therefore requiring control strategies. These include intake temperature control (Chia-Jui Chiang et al., 2012), valve control (Yeom et al., 2007), and fuel control (Bidarvatan and Shahbakhti, 2013). Dual-fuel control uses two fuels with different combustion reactivity. By changing the proportion of fuel injected the combustion timing can be altered. A control strategy must be implemented like MPC (Ebrahimi and Koch, 2015), or PI (Strandh et al., 2004). This paper investigates the use of an Iterative Learning Controller (ILC). ILC's are useful for repetitive processes like robotics (Parzer et al., 2015), and machining (Fiorentino et al., 2015). Several surveys have been done to highlight the current ILC knowledge and its strength and weaknesses (Bristow et al., 2006) (Moore et al., 2006) and (Wang et al., 2009). A norm-optimal control has been developed by Barton and Alleyne (2011). Several papers have investigated its convergence and robustness using worst-case norm optimal (Son et al., 2015), Linear Matrix Inequality (LMI) (Gauthier and Boulet, 2005) and (Galkowski et al., 2003), and interval values (Ahn et al., 2007).

ILC is useful for systems that are repetitive. These include electromagnetic valve control (Tsai et al., 2012), and Diesel combustion control (Hinkelbein et al., 2010). Dooren (2015) used an ILC to control multiple aspects of an spark ignition engine. An ILC can find the ideal input sequence for a process that is repetitive. ILC control has been shown to work well for systems with minimal system information (Ahn et al., 2007) and is easy to design. Any engine application that requires repetitive operation will be ideally suited for ILC implementation. This may include idle speed control for disturbance rejection, load changes for generator applications or even en route performance optimization for mass transit systems similar to the work done in Kapania and Gerdes (2015) which used an ILC for path optimization for an autonomous vehicle. A detailed description on how ILC works is given in Ahn et al. (2007). The application of an ILC to HCCI is the subject of this paper. Here the CFR engine is operated over repetitive load and combustion timing steps.

2. EXPERIMENTAL SETUP

The engine used is a modified Cooperative Fuels Research (CFR) which is often used for Octane testing. The advantage of this engine is the compression ratio can easily be altered. The standard CFR engine is modified as follows: head replacement, addition of two port injectors, and an intake air heater. The head has ports for both an in-cylinder pressure transducer, Kistler 6043A piezoelectric pressure, and a jacket temperature thermocouple. The

^{*} Financial support for this research provided by Biofuelnet Canada.

Table 1. Engine Specifications

Engine Parameter	Value/Type
combustion chamber	pancake with flat-top piston
engine type	water cooled
number of cylinders	1
displacement	612 cm ³
bore	82.6 mm
stroke	114.3 mm
compression ratio	variable from 4 to 18

Table 2. Engine Description

Label	Description
1	Air Flow meter
2	Intake Plenum
3	Intake Heater
4	Throttle
5	Intake Manifold
6	Fuel Injectors
7	EGR valve
8	Combustion Chamber
9	Lambda Sensor

engine specifications are given in table 1. A schematic of the setup is given in Fig. 1 with P denoting a pressure measurement port and T denoting thermocouple location. The components are listed in table 2 and the operating parameters for all tests are given in table 3.

Intake pressure, in-cylinder pressure and torque are collected on a 0.1° basis using a crank shaft encoder with a NI card PCIe-6431. All other data is collected at 10 Hz using two NI PCI-MIO-16E and a NI USB-6225. Labwindows/CVI is the platform used for data collection and control implementation. The CVI program communicates the injector opening time to an Arduino Due. A Tec GT ECU then relays the injector timing to the Arduino which then controls the injectors.

The system outputs are crank angle after top dead center when 50% of the mass fraction is burned (CA50) and the gross indicated mean effective pressure (IMEP). These are calculated from the pressure trace as:

$$dQ = \frac{\gamma}{\gamma-1} PdV + \frac{1}{\gamma-1} VdP \quad (1)$$

$$IMEP = \frac{1}{V_d} \int_{IVC}^{EVO} PdV \quad (2)$$

with Q being the chemical energy released from the fuel, γ is ratio of specific heats of the gas, P is the in-cylinder pressure, V is the in-cylinder volume and V_d is the displacement volume. Eqn. 1 assumes that none of the energy released from combustion is lost. Heat transfer to the walls and crevice losses are ignored to reduce the calculation time. CA50 is found by integrating dQ from IVC to EVO and finding θ when $Q(\theta) = Q_{max}/2$.

The system inputs are amount of iso-octane, E_{iso} , and n-heptane, E_{hept} , injected into the manifold. The injected energy is controlled by the opening time of the injectors. A calibration is found (Slepicka, 2016) to relate the injected energy to opening time.

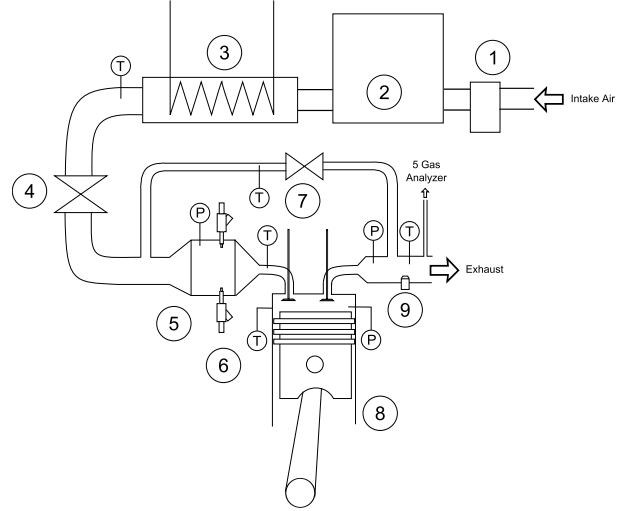


Fig. 1. Engine Schematic

Table 3. Operating Parameters

Parameter	Value
Intake Temperature	100°C
Intake Pressure	Atmospheric (92 to 94 kPa)
Speed	800 RPM
Compression Ratio	11:1

3. ILC SETUP

Given a system plant P :

$$P \equiv \begin{cases} x_j(k+1) = A(k)x_j(k) + B(k)u_j(k) \\ \delta y_j(k) = C(k)x_j(k) + D(k)u_j(k) \end{cases} \quad (3)$$

$$y_j(k) = \delta y_j(k) + y_o(k) + d_j(k) \quad (4)$$

With $x \in \mathbb{R}^n$ being the system states, $u \in \mathbb{R}^m$ contains the inputs, and $y \in \mathbb{R}^p$ contains the outputs where j is the iteration index, k is the time step in the iteration or “pass”. P can be written as a block matrix:

$$P = \begin{bmatrix} H_{0,0} & & 0 \\ \vdots & \ddots & \\ H_{N-1,0} & \cdots & H_{N-1,N-1} \end{bmatrix} \quad (5)$$

With N being the number of time steps per iteration and $d_j \in \mathbb{R}^p$ is the disturbance. For Linear Time Invariant (LTI) system:

$$H_{i,l} : \begin{cases} D, & i = l \\ CA^{l-i-1}B, & l > i \end{cases} \quad (6)$$

Now assuming $D = 0 \in \mathbb{R}^{p \times m}$ as there is no feed through in the system we are investigating, P becomes:

$$P = \begin{bmatrix} 0 & \cdots & 0 \\ H(1) & 0 & \vdots \\ H(2) & H(1) & 0 \\ \vdots & & \ddots \\ H(N-1) & \cdots & H(1) & 0 \end{bmatrix} \quad (7)$$

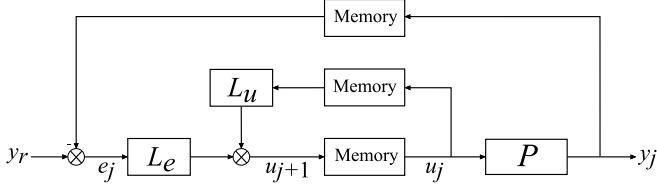


Fig. 2. ILC block diagram

Where $H(i) \in \mathbb{R}^{p \times m}$ is the i^{th} impulse response term. This makes $P \in \mathbb{R}^{pN \times mN}$. The system can be written into a lifted form as (Barton and Alleyne, 2011):

$$\mathbf{y}_j = P\mathbf{u}_j + \mathbf{d}_j \quad (8)$$

Where

$$\mathbf{u}_j = \begin{bmatrix} u_j(0) \\ u_j(1) \\ \vdots \\ u_j(N-1) \end{bmatrix} \quad \mathbf{u}_j(k) = \begin{bmatrix} u_j^{(1)}(k) \\ \vdots \\ u_j^{(m)}(k) \end{bmatrix} \quad (9)$$

$$\mathbf{y}_j = \begin{bmatrix} y_j(0) \\ y_j(1) \\ \vdots \\ y_j(N-1) \end{bmatrix} \quad \mathbf{y}_j(k) = \begin{bmatrix} y_j^{(1)}(k) \\ \vdots \\ y_j^{(p)}(k) \end{bmatrix} \quad (10)$$

This is also known as a ‘‘super-vector’’ rearrangement as $\mathbf{u}_j \in \mathbb{R}^{mN}$ and $\mathbf{y}_j \in \mathbb{R}^{pN}$ becomes a vector containing each time step’s input and output for the j^{th} iteration. The iteration error, \mathbf{e}_j , given a reference trajectory \mathbf{y}_r , is defined as:

$$\mathbf{e}_j = \mathbf{y}_r - \mathbf{y}_j \quad (11)$$

A generalized ILC can then be implemented as, (Barton and Alleyne, 2011):

$$\mathbf{u}_{j+1} = L_u \mathbf{u}_j + L_e \mathbf{e}_j \quad (12)$$

L_e and L_u are termed the learning and forgetting filters, respectively. A block diagram showing this control strategy is given in Fig. 2. The memory blocks are used to save the entire iteration’s data of its respective input. The purpose of the ILC control design is to eliminate each time step’s error using the previous iteration’s error and input. There are many ways to design L_e and L_u (Bristow et al., 2006). One example is a norm optimal approach proposed by Barton and Alleyne (2011). This procedure requires positive definite matrices Q , S and R to be selected. These matrices are weightings for the control design with $Q \in \mathbb{R}^{pN \times pN}$ weighting the error, $S \in \mathbb{R}^{mN \times mN}$ weighting the input, and $R \in \mathbb{R}^{mN \times mN}$ weighting the change in input between the iterations. If they are selected as $Q = qI$, $R = rI$, and $S = sI$ then only q , s , $r \in \mathbb{R}$ need to be selected. Solving the norm optimal control L_e and L_u are:

$$L_u = (P^T Q P + S + R)^{-1} (P^T Q P + R) \quad (13)$$

$$L_e = (P^T Q P + S + R)^{-1} P^T Q \quad (14)$$

This paper also investigates new method for designing L_e with minimal system information. It requires finding the

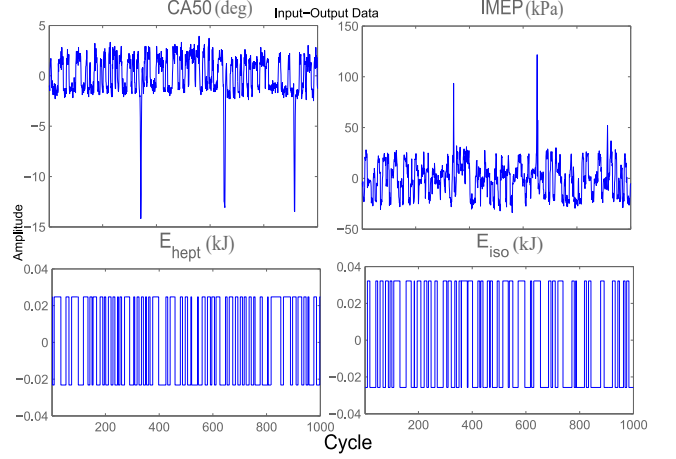


Fig. 3. CFR engine response from RBS input with mean removed.

steady-state Jacobian, $J \in \mathbb{R}^{m \times m}$, of the system, assuming $m = p$. It also requires the Jacobian is invertible. Then populating the off-diagonal in an Arimoto-like manner (Ahn et al., 2007):

$$L_e = \begin{bmatrix} 0 & K \cdot J^{-1} & 0 & 0 \\ 0 & 0 & K \cdot J^{-1} & \ddots \\ & \ddots & \ddots & \ddots \end{bmatrix} \quad (15)$$

Where $K > 0 \in \mathbb{R}$ can be decreased to ensure stability or increased to speed up convergence. The purpose of having it the off-diagonal is $u_j(k)$ affects $y_j(k+1)$ due to $D = 0$ in Eqn. 6. The forgetting filter is made equal to the identity matrix, $L_u = I$, to ensure zero steady-state error and rapid convergence. This method will be denoted as ‘‘model-less’’ control.

For the CFR engine HCCI control k represents the combustion cycle in one iteration or ‘‘pass’’, and $m = p = 2$ so:

$$\mathbf{u}_j(k) = \begin{bmatrix} E_{hept}(k) \\ E_{iso}(k) \end{bmatrix}, \quad \mathbf{y}_j(k) = \begin{bmatrix} CA50(k) \\ IMEP(k) \end{bmatrix} \quad (16)$$

Since the ILC considers the system one iteration at a time, ‘non-casual’ algorithms can be applied within the iteration. Filters that utilizes future inputs like a zero-phase filter or a Gaussian filter are used. The zero-phase filter has the benefit of cutting out specific frequencies without causing any phase lag. The Gaussian filter has the benefit of no overshoot with a minimal rise-time. Both are investigated in this paper.

4. SYSTEM IDENTIFICATION

Using Matlab system identification software, the parameters of a linear model, P in Eqn. 3, are obtained. For accurate model identification the input must have persistent excitation so a Pseudo Random Binary Signal (PRBS) is generated and input to the engine. The results with mean removed are shown in Fig. 3. Three cycles can be seen to have early combustion compared to the rest. These are considered outliers and removed from the data as they

Table 4. ARMAX polynomial orders.

Order	Polynomial
1	$A_{12}, A_{21}, A_{22}, B_{12}, B_{22}$
2	A_{11}, B_{11}
3	B_{21}, C_1, C_2

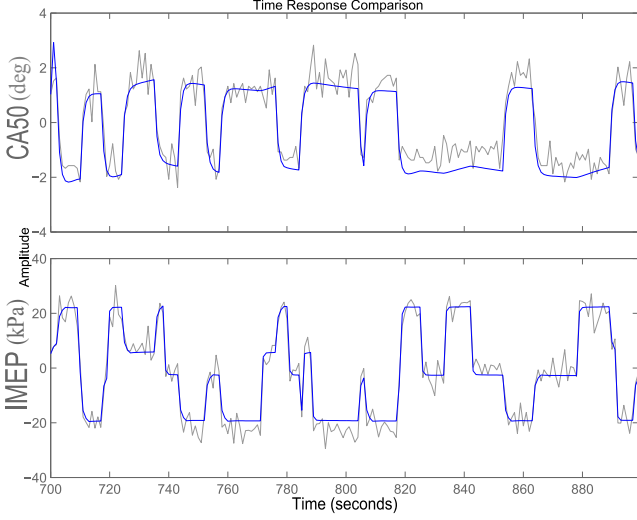


Fig. 4. ARMAX simulation comparison to CFR engine data.

are due to an anomaly of the engine to knock every few hundred cycles.

Using an ARMAX model as below:

$$\mathbf{A}(z)y_j(k) = \mathbf{B}(z)u_j(k) + \mathbf{C}(z)d_j(k) \quad (17)$$

where $y_j(k)$ and $u_j(k)$ are given in Eqn. 16 and:

$$\mathbf{A}(z) = \begin{bmatrix} A_{11}(z) & A_{12}(z) \\ A_{21}(z) & A_{22}(z) \end{bmatrix} \quad (18)$$

$$\mathbf{B}(z) = \begin{bmatrix} B_{11}(z) & B_{12}(z) \\ B_{21}(z) & B_{22}(z) \end{bmatrix} \quad (19)$$

$$\mathbf{C}(z) = \begin{bmatrix} C_1(z) & 0 \\ 0 & C_2(z) \end{bmatrix} \quad (20)$$

the delay of the system was found to be 1, which agrees with the $D = 0$ assumption and physical intuition. The orders of the system are chosen to obtain the best fit. The system polynomials are given in table 4. The fit for CA50 is 61.25% and IMEP is 77.58% on the validation data. The results are given in Fig. 4.

The ARMAX model, can be represented as system P in Eqn. 7, and is used to find the norm optimal control using Eqns. 13 and 14.

5. ILC COMPARISON

Noise in the outputs gives standard deviations of 0.424 CAD and 3.98 kPa for CA50 and IMEP, respectively. These are found from the flat reference signal sections of the engine response given in Fig. 7. To account for the noise, the r value in the norm optimal control needs to be large enough to ensure the noise does not transfer to the input but not to large to impact convergence. Since r , q , and s are weightings, their values are relative to each other,

i.e. if all three were doubled this would have no effect on the response. From this, $q = 1$ is the reference point as it weights the error and $s = 0.1$ to ensure that it has minimal effect while stopping the input from diverging too much. The r value is increased in simulation until convergence speed is noticeably reduced, which gives an $r = 3000$. The model-less control's K is set to 0.75 to ensure convergence. The Jacobian, J , was found by selecting a base operating point, $E_{hept} = 0.480$ kJ and $E_{iso} = 0.163$ kJ, and changing the input, u in Eqn. 16, and recording the steady state output, y in Eqn. 16. Twenty three such operating points were tested to find the slope around the base operating point. A 2-D linear regression was performed resulting in:

$$\begin{bmatrix} CA50_{ss} \\ IMEP_{ss} \end{bmatrix} = \begin{bmatrix} -114 & -15.3 \\ 463 & 467 \end{bmatrix} \begin{bmatrix} E_{hept} \\ E_{iso} \end{bmatrix} + \begin{bmatrix} 66.1 \\ -1.11 \end{bmatrix} \quad (21)$$

With $R^2 = 0.987$ and 0.876 for IMEP and CA50, respectively. Points with $CA50 \leq 0$, i.e. before top dead center, are ignored.

A reference step signal in IMEP from 280 to 350 kPa at cycle 20 and a CA50 step from 3 to 6 CAD aTDC at cycle 40 are used to experimentally test each control type, model-less and norm optimal, with each filter, Gaussian, Zero-phase and filter-less on the CFR engine. The jump in IMEP is chosen as it the maximum range the engine can operate at; higher IMEP causes knock and lower the engine cannot overcome the friction losses. The normalized RMS error for each trial is given in Fig. 5. IMEP is consistent in each test; It converges quickly and is stable. CA50 converges much faster in the model-less control and has the most stable convergence with the Zero-phase filter. The error for IMEP is given in Fig. 6 for the first 5 iterations of the model-less control with zero-phase filtering. The final control signals are given in Fig. 7. For norm-optimal control with filters the r value is decreased to 0.1 to speed up convergence as the filter is designed to minimize the noise. For each control style the same initial iteration input was used, therefore the normalized error can be compared between each control style. One issue that arises from the current control strategy is the inability to recover from a misfire without additional control logic.

6. PI COMPARISON

Two standard PI controllers are implemented to control CA50 using n-heptane and IMEP using iso-octane since they have the strongest correlations. This is seen in Fig 8 by the initial response and final value observed in the step responses between each input and output. To provide a simple PI control comparison interactions between the two controllers are ignored and considered disturbances. The gains are initially set using simulation but are tuned during engine operation until near deadbeat control is found. The control and response are given in Fig. 9.

Finally the error from the tuned PI are compared to the best ILC case, the model-less with zero-phase filtering. Both are normalized with the first ILC iteration error. Fig. 10 shows the comparison and how, after 3 iterations, the ILC outperforms the PI and converges to a smaller value.

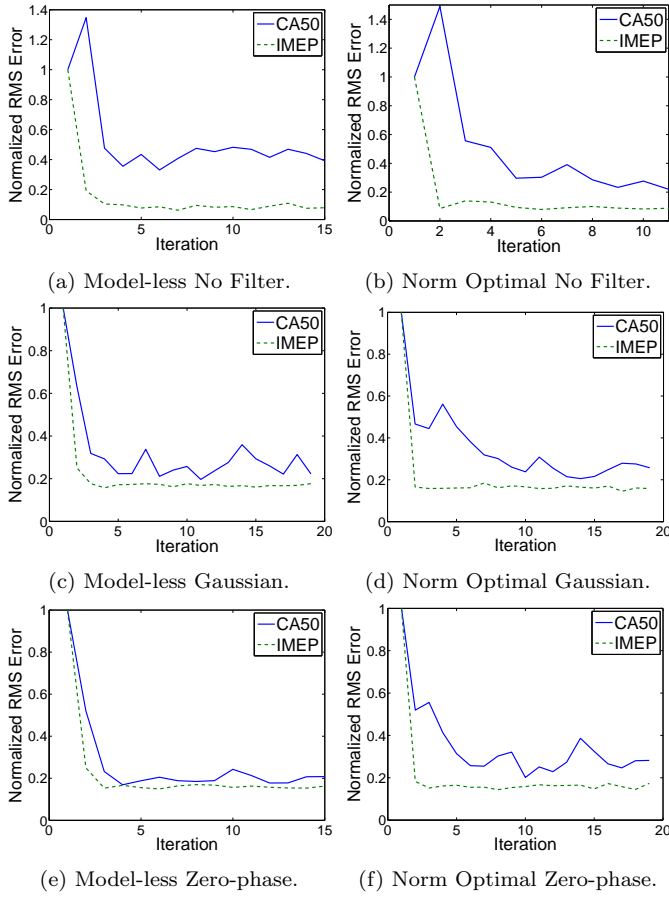


Fig. 5. Normalized RMS error from CFR engine response.

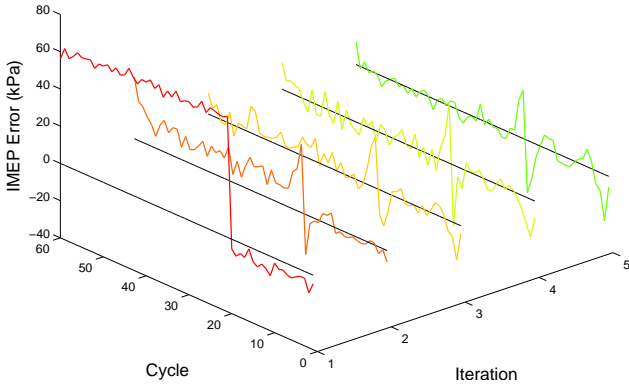


Fig. 6. Iteration error for IMEP on Model-less control with Zero-phase filter on CFR engine.

7. CONCLUSION

The ILC performs well for repetitive control of CA50 and IMEP in HCCI on a CFR engine. An Arimoto-like control structure using a steady-state Jacobian is found to be superior to a norm optimal approach. The noise was transferred through the controller necessitating the need for a filter. Two non-causal filters are investigated, a zero-phase and a Gaussian filter. The best filter is found to be zero-phase filter which outperforms the Gaussian in both convergence speed and final iteration RMS error. The best ILC, model-less with zero-phase filter, is compared to a PI controller. The ILC is found to have less RMS error than the PI after 3 iterations. An ILC to find optimal input

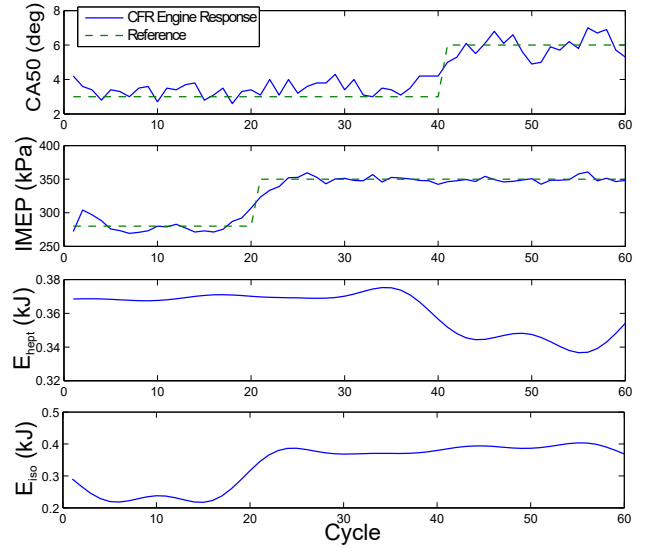


Fig. 7. Final iteration control signals for Model-less control with Zero-phase filter.

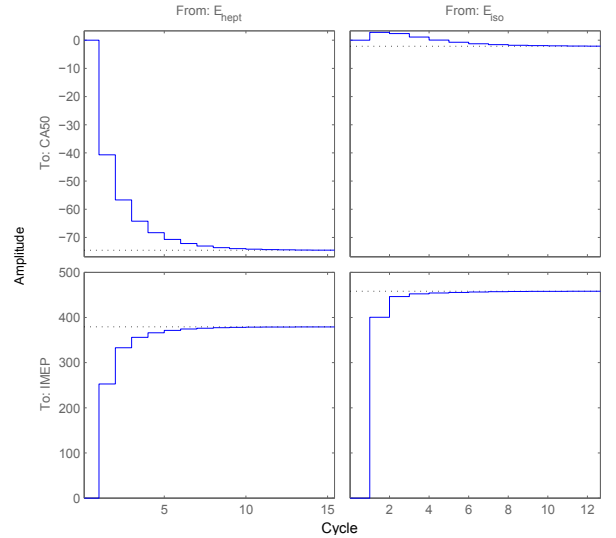


Fig. 8. Step responses from ARMAX model.

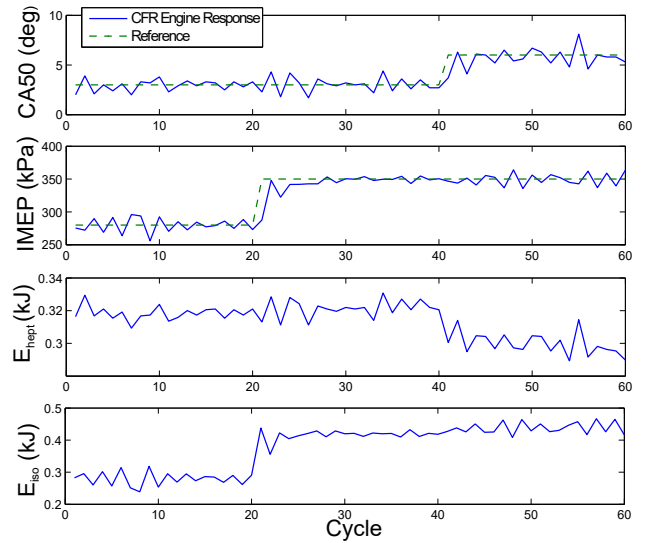


Fig. 9. PI control signals.

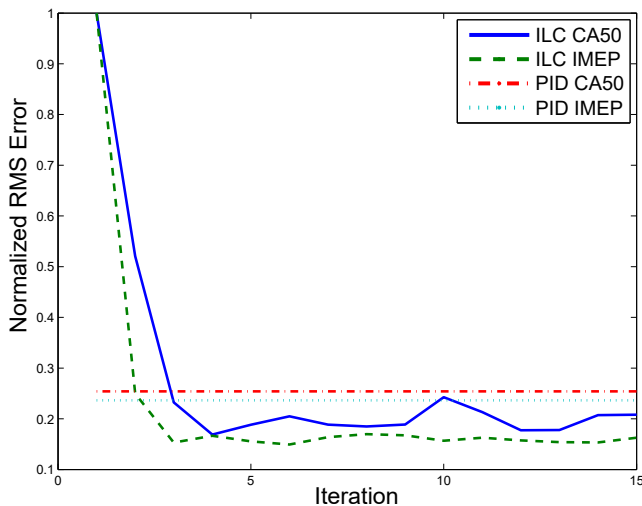


Fig. 10. Normalized RMS errors for ILC control and PI results from CFR engine.

can be used as a feed-forward strategy for HCCI control of a cyclic reference trajectory to reduce error. Since the ultimate input is found and saved, it can be used in look-up table strategies.

Future work for this project includes augmenting the ILC with feedback to reduce the error in the first few iterations and testing the trade-off in the model-less control by varying the number of data points needed to get an accurate Jacobian. The robustness of the control at various operating points and with alternative fuels is also planned.

REFERENCES

- Ahn, H.S., Moore, K.L., and Chen, Y. (2007). Stability analysis of discrete-time iterative learning control systems with interval uncertainty. *Automatica*, 43(5), 892–902.
- Barton, K.L. and Alleyne, A.G. (2011). A norm optimal approach to time-varying ILC with application to a multi-axis robotic testbed. *IEEE Transactions on Control Systems Technology*, 19(1), 166–180.
- Bidarvatan, M. and Shahbakhti, M. (2013). Two-Input Two-Output Control of Blended Fuel HCCI Engines. 2013-01-1663.
- Bristow, D., Tharayil, M., and Alleyne, A. (2006). A Survey of Iterative Learning Control. *IEEE Control Systems Magazine*, 26(3), 96–114.
- Chia-Jui Chiang, Chih-Cheng Chou, and Jian-Hong Lin (2012). Adaptive control of homogeneous charge compression ignition (HCCI) engines. In *2012 American Control Conference (ACC)*, 21, 2066–2071. IEEE.
- Dooren, S.V. (2015). *Iterative Learning Control for Internal Combustion Engines*. Master's, Institute for Dynamic Systems and Control Swiss Federal Institute of Technology (ETH) Zurich.
- Ebrahimi, K. and Koch, C.R. (2015). Model Predictive Control for Combustion Timing and Load Control in HCCI engines. *SAE*, 2015-01-08.
- Fiorentino, A., Giardini, C., and Ceretti, E. (2015). Application of artificial cognitive system to incremental sheet forming machine tools for part precision improvement. *Precision Engineering*, 39, 167–172.
- Galkowski, K., Lam, J., Rogers, E., Xu, S., Sulikowski, B., Paszke, W., and Owens, D. (2003). LMI based stability analysis and robust controller design for discrete linear repetitive processes. *International Journal of Robust and Nonlinear Control*, 13(13), 1195–1211.
- Gauthier, G. and Boulet, B. (2005). Convergence analysis of terminal ILC in the z domain. In *Proceedings of the 2005, American Control Conference, 2005.*, 184–189. IEEE.
- Hinkelbein, J., Sandikcioglu, C., Pischinger, S., Lamping, M., and Körfer, T. (2010). Control of the diesel combustion process via advanced closed loop combustion control and a flexible injection rate shaping tool. *SAE International Journal of Fuels and Lubricants*, 2(2), 362–375.
- Iida, M., Hayashi, M., Foster, D.E., and Martin, J.K. (2003). Characteristics of Homogeneous Charge Compression Ignition (HCCI) Engine Operation for Variations in Compression Ratio, Speed, and Intake Temperature While Using n-Butane as a Fuel. *Journal of Engineering for Gas Turbines and Power*, 125(2), 472–478.
- Kalghatgi, G.T. and Head, R.A. (2004). The Available and Required Autoignition Quality of Gasoline - Like Fuels in HCCI Engines at High Temperatures. In *Spring Fuels and Lubricants Conference and Exhibition, 2004-01-1969*.
- Kapania, N.R. and Gerdes, J.C. (2015). Path tracking of highly dynamic autonomous vehicle trajectories via iterative learning control. In *2015 American Control Conference (ACC)*, 2753–2758. IEEE.
- Moore, K.L., Chen, Y., and Ahn, H.S. (2006). Iterative Learning Control: A Tutorial and Big Picture View. In *Proceedings of the 45th IEEE Conference on Decision and Control*, 2352–2357. IEEE.
- Parzer, H., Gattringer, H., Müller, A., and Naderer, R. (2015). Learning Robot Force/Position Control for Repetitive High Speed Applications with Unknown Non-Linear Contact Stiffness. *Pamm*, 15(1), 65–66.
- Slepicka, C. (2016). *Iterative Learning Control for Fuel Robust HCCI*. Master's thesis, University of Alberta.
- Son, T., Pipeleers, G., and Swevers, J. (2015). Robust Monotonic Convergent Iterative Learning Control. *IEEE Transactions on Automatic Control*, 32, 1–1.
- Strandh, P., Bengtsson, J., Johansson, R., Tunestål, P., and Johansson, B. (2004). Cycle-to-Cycle Control of a Dual-Fuel HCCI Engine. In *SAE Technical Paper*, volume 01.
- Tsai, J., Koch, C.R., and Saif, M. (2012). Cycle Adaptive Feedforward Approach Controllers for an Electromagnetic Valve Actuator. *IEEE Transactions on Control Systems Technology*, 20(3), 738–746.
- Wang, Y., Gao, F., and Doyle, F.J. (2009). Survey on iterative learning control, repetitive control, and run-to-run control. *Journal of Process Control*, 19(10), 1589–1600.
- Yeom, K., Jang, J., and Bae, C. (2007). Homogeneous charge compression ignition of LPG and gasoline using variable valve timing in an engine. *Fuel*, 86(4), 494–503.